PHYSICAL REVIEW A VOLUME 21, NUMBER 3 MARCH 1980

Kinetics of nucleation in near-critical fluids

J. S. Langer and A. J. Schwartz
Physics Department, Carnegie-Mellon University, Pittsburgh, Pennsylvania 15213
(Received 24 September 1979)

A simple set of rate equations is proposed to describe nucleation and growth of droplets in metastable, near-critical fluids. These equations are used in conjunction with steady-state nucleation theory to compute completion times for phase separation in binary mixtures. Reexamination of available experimental data provides little if any evidence for the major failure of conventional nucleation theory that has been postulated on the basis of these data.

I. INTRODUCTION

Near-critical fluids, either pure substances or simple binary mixtures, should be ideal systems for study of the kinetics of first-order phase transformations. Fluids can be highly purified, and they support no internal strains or similar defects. By working near a critical point, one can deal with phenomena which occur over large lengths and long times and which therefore can be described by universal laws of diffusion and flow without reference to specific molecular properties. Thus it should be possible to test some of the most fundamental concepts of nonequilibrium statistical mechanics by observing, say, the separation of phases in a supersaturated solution near its critical concentration or the condensation of a supercooled vapor near its critical density. A number of experiments of this kind have been performed in recent years.[1-4] Essentially without exception, nucleation measurements performed in the critical region have indicated dramatic differences between theory and experiment. The purpose of the present investigation is to devise a more detailed theoretical description of the actual experimental situation and thus to see which aspects of the theory, if any, are really in disagreement with the observations.

Theories of nucleation[5] ordinarily predict the rate of formation of stable embryos, i.e., droplets, of an emerging phase as a function of the degree of supersaturation in an initially homogeneous metastable system. This function usually turns out to vary extremely rapidly and to pass through observable rates in a narrow range of supersaturations, thus effectively defining a limit of metastability. It is this limit which has been measured and found to exceed the predicted value by factors of 2 or more in the critical region. That is, critical systems seem to possess an anomalously high degree of stability, the conventional nucleation mechanism seems somehow to be suppressed in a situation where one would have thought the theory would be most accurate.

A basically very simple possibility for the resolution of this paradox has been suggested by Binder and Stauffer[6] in a short note toward the end of one of their recent papers about droplet kinetics. These authors argue that the experimentally meaningful quantity is not the nucleation rate itself but the time required for the reaction to go to completion. To estimate a completion time, one must consider droplet growth as well as formation. Because the growth of droplets is controlled by diffusion—the experiments of interest have been performed in systems where the relevant order parameter is a locally conserved quantity—and diffusive processes over critical length scales become very slow near the critical point, the overall reaction rates may be appreciably different from estimates based on nucleation alone. Binder and Stauffer show that a relatively simple calculation along these lines indicates at least a possibility of reconciling theory with experiment. [A specific statement of the Binder-Stauffer theory will be found in Eqs. (4.2)–(4.5).]

The calculation which we describe is an attempt to carry out the Binder-Stauffer program, that is, to predict in some detail the complete sequence of states of a phase-separating fluid starting from the quench into a supersaturated state and ending with completion of the reaction. This is an intrinsically difficult problem because the stochastic aspects of a first-principles nucleation theory seem to require a mathematical formulation which is not convenient for the description of late-stage growth processes. Our policy will be to keep the calculation as simple and intuitive as possible, which means that we use a droplet model throughout. To do this, however, we must introduce several inelegant assumptions regarding statistical properties of the system. As a result, our predictions are not as compelling as we would like; but at least they should serve as a guide to further experimentation.

Our theory most nearly corresponds to that of

Binder and Stauffer in the limit of small supersaturation, where droplet activation energies are of the order of $20kT$ or larger. Here the nucleation rate is slow, and completion of the reaction occurs only when a relatively small number of embryos have grown to macroscopic size. The one novel point that emerges from our time-dependent calculation is that the reaction may not appear to start until some time after the quench. This regime of small supersaturation is the one in which experimentalists report seeing no reaction at all. In view of the new calculations, it seems possible that they have not looked closely enough or waited long enough.

At larger supersaturations, where activation energies are of the order of $10kT$ or smaller, our theory predicts a qualitatively different behavior. Here nucleation is occurring rapidly, and droplet growth is relatively slow. When we account for the fact that the smaller droplets tend to dissipate rather than grow—the Lifshitz-Slyozov effect[7]—we find an overall reaction rate which is very much smaller than what one might have estimated on the basis of nucleation alone. The system creeps toward completion in a state in which droplets of about the critical size are appearing and disappearing at nearly identical rates. In a crude sense the process we are describing here is the extreme nonlinear version of spinodal decomposition.[8]

II. BASIC INGREDIENTS

In this section we summarize the various thermodynamic and kinetic formulas which will be the basic ingredients of our theory.

For simplicity, we consider only the case of phase separation in a simple two-component fluid. (It is not difficult to substitute heat content for chemical composition in order to use the same analysis for pure substances.) A schematic phase diagram is shown in Fig. 1. Here C denotes the concentration of one of the components which we call the "solute." The initial metastable system is assumed to be prepared at temperature T and uniform concentration C_1 by quenching through a temperature δT. Because all processes will be assumed to occur isothermally at T, it will be more convenient to use the temperature variable $\epsilon = 1 - T/T_c$ associated with the quenched state rather than the quantity $\tilde{\epsilon}$, shown in Fig. 1, which is more common in the experimental literature. The relation between the two quantities is simply

$$\epsilon = \tilde{\epsilon} + \delta T/T_c . \tag{2.1}$$

In the limit of very shallow quenches, $\delta T/\epsilon T_c \ll 1$, the two ϵ's are almost identical. Recent experiments[4] explore the region where $\delta T/\epsilon T_c$ is of the order of unity, however, so we must be careful.

As shown in Fig. 1, C_A and C_B are the equilibrium values of C for two-phase coexistence at T, $\Delta C = C_B - C_A$ is the miscibility gap, and $\delta C_1 = C_1 - C_A$ is the initial supersaturation. We use square brackets to denote critical amplitudes, and conventional notation and scaling laws for critical exponents.[9] Thus,

$$\Delta C = [\Delta C]\epsilon^{\beta} . \tag{2.2}$$

If we assume that the coexistence curve is given by

$$C_A \cong C_{\text{crit}} - \tfrac{1}{2}[\Delta C]\epsilon^{\beta} , \tag{2.3}$$

then the relation between initial supersaturation and quench depth is

$$\frac{\delta C_1}{\Delta C} = \frac{1}{2}\left[1 - \left(1 - \frac{\delta T}{\epsilon T_c}\right)^{\beta}\right] = \frac{1}{2}\left[1 - \frac{1}{(1+\delta T/\tilde{\epsilon} T_c)^{\beta}}\right] . \tag{2.4}$$

The appropriate scaling variable for measuring supersaturation is $\delta\mu/\epsilon^{\beta\delta}$, where δ is the usual exponent associated with the critical isotherm and $\delta\mu$ is the chemical potential per solute molecule measured from its two-phase equilibrium value. In the absence of a detailed equation of state in the metastable region, we use the approximation

$$\delta\mu \cong \frac{\partial \mu}{\partial C_A}\delta C , \tag{2.5}$$

where $\partial\mu/\partial C_A$ is independent of C. (Perhaps it would be better to use a Ginzburg-Landau "ϕ^4" approximation of the form

$$\delta\mu \cong \frac{\partial \mu}{\partial C_A}\delta C\left(1 - \frac{\delta C}{\Delta C}\right)\left(1 - \frac{2\delta C}{\Delta C}\right),$$

but it seems to us that the accuracy of the present theory does not warrant this extra complication.) Note that the symbols $\delta\mu$ and δC, without subscripts, denote arbitrary supersaturations in the

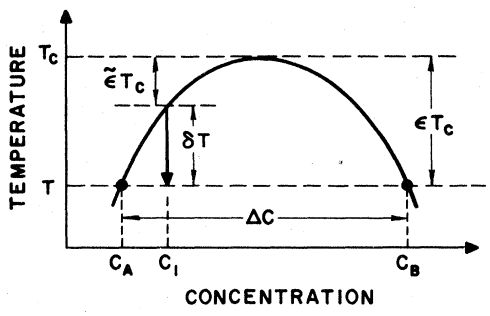

FIG. 1. Schematic phase diagram showing coexistence curve and relevant quantities defined in the text.

A phase and are not necessarily related to the initial quench depth via Eq. (2.4). It is convenient to define the dimensionless variable

$$x \equiv \frac{2}{\beta(\partial\mu/\partial C_A)(\Delta C)}\frac{\delta\mu}{\epsilon^{\beta\delta}} \cong \frac{2}{\beta}\frac{\delta C}{\Delta C}. \tag{2.6}$$

Experimental data usually are reported in terms of

$$\tilde{x}_1 \equiv \delta T/\bar{\epsilon} T_c, \tag{2.7}$$

so that the initial value of x is

$$x_1 = (1/\beta)[1 - 1/(1+\tilde{x}_1)^{\beta}], \tag{2.8}$$

and $x_1 \cong \tilde{x}_1$ for small $\tilde{x}_1$.

Consider now a unit volume of our system at some time after the quench, such that the reaction has gone part of the way toward completion. We assume that the system consists of droplets of B phase immersed in an A phase whose supersaturation has been reduced from δC_1 to δC. The number of solute molecules is conserved; therefore, by use of the lever rule, the volume fraction occupied by B-phase droplets must be

$$\frac{\delta C_1 - \delta C}{\Delta C - \delta C} \cong \tfrac{1}{2}\beta(x_1 - x) \cong \tfrac{4}{3}\pi \bar{R}^3 N, \tag{2.9}$$

where N is the number of droplets per unit volume and $\bar{R}$ is their average radius.

A spherical droplet of radius R and uniform concentration C_B, immersed in A phase with a small supersaturation δC, will grow at the rate

$$\frac{dR}{dt} \cong \frac{D}{R}\left(\frac{\delta C}{\Delta C} - \frac{2d_0}{R}\right), \tag{2.10}$$

where D is the diffusion constant and d_0 is a capillary length proportional to the surface tension σ,

$$d_0 = \sigma \Big/ \left[(\Delta C)^2 \frac{\partial\mu}{\partial C_A}\right]. \tag{2.11}$$

In a "ϕ^4" theory we have simply

$$d_0 = \tfrac{1}{6}\xi, \tag{2.12}$$

where ξ is the correlation length in the A phase. Equation (2.12) is a convenient and apparently fairly accurate first approximation and we use it frequently in what follows. Note that the right-hand side of (2.10) changes sign at the critical radius R^*:

$$R^* = \frac{2d_0(\Delta C)}{\delta C} = \frac{4d_0}{\beta x} \cong \frac{2\xi}{x}. \tag{2.13}$$

We have used (2.12) and $\beta \cong \frac{1}{3}$ in the final approximate form of (2.13).

Equations (2.9), (2.10), and (2.13) are the basis of the Lifshitz-Slyozov[7] theory, which describes droplet growth during the late stages of phase separation after nucleation of new droplets has ceased. The essential ingredient of our own theory, of course, is the nucleation rate. We base our analysis on the field-theoretic version of nucleation theory,[10-14] which starts from the relation[11]

$$J = (\kappa/\pi kT)\,\mathrm{Im}f(\epsilon, \delta\mu). \tag{2.14}$$

Here J is the nucleation rate per unit volume, Imf is the imaginary part of the analytic continuation of the free-energy density to metastable values of the chemical potential, and κ is a kinetic factor given, for our purposes, by

$$\kappa = \frac{d}{dt}\ln(R - R^*)\Big|_{R=R^*} = \frac{2Dd_0}{(R^*)^3} \cong \frac{1}{24}\frac{D\chi^3}{\xi^2}. \tag{2.15}$$

Equation (2.14) has been derived systematically only in the limit of small $\delta\mu$; but we presume—in the absence of a better theory—that it continues to make sense at moderately large values of the supersaturation.

The evaluation of Imf has been discussed in widely differing contexts throughout the literature. In the limit of small $\delta\mu$ it is believed to have the form[15]

$$\frac{1}{kT}\mathrm{Im}f \approx \frac{A}{\xi^3}\left(\frac{x_0}{x}\right)^{7/3}\exp\left[-\left(\frac{x_0}{x}\right)^2\right], \tag{2.16}$$

where x is proportional to $\delta\mu/\epsilon^{\beta\delta}$ according to (2.6), ξ is the ϵ-dependent correlation length, and A and x_0 are dimensionless constants. The quantity $(x_0/x)^2$ is the activation energy ΔE^* in the conventional droplet model; that is,

$$\frac{\Delta E^*}{kT} = \frac{4\pi\sigma R^{*2}}{3kT} = \frac{64\pi\sigma d_0^2}{3kT\beta^2 x^2} \equiv \left(\frac{x_0}{x}\right)^2, \tag{2.17}$$

so that

$$x_0 = \frac{8}{\beta}\left(\frac{\pi}{3}\right)^{1/2}\left[\frac{\sigma d_0^2}{kT}\right]^{1/2} \cong 4\left[\frac{\sigma\xi^2}{kT_c}\right]^{1/2}. \tag{2.18}$$

The parameter x_0 is known to be of the order of unity for the substances of interest here. We shall say more about specific values of x_0 in Sec. V. It is possible to estimate only the order of magnitude of the constant A in (2.16). An approximation based on Eq. (4.13) in Ref. 14 yields

$$A \cong \frac{1}{3\sqrt{3}}\left[\frac{\sigma\xi^2}{kT_c}\right]^{3/2}\left(\frac{2}{3\beta}\right)^4 \cong \frac{x_0^3}{12\sqrt{3}}, \tag{2.19}$$

where we have evaluated the capillary term so as to be consistent with (2.18), but this estimate omits unknown logarithmic corrections to the activation energy. The factor $(x_0/x)^{7/3}$ arises in part from such corrections. For details see Günther *et al.*[15]

Equation (2.16) is qualitatively incorrect for large values of x because it disagrees with the

scaling form of f:

$$f \approx \epsilon^{3\nu}(-x)^{1+1/\delta}, \quad x \gg 1. \tag{2.20}$$

Analytic continuation of (2.20) to large positive (metastable) values of x requires that $\mathrm{Im}f$ be proportional to $x^{1+1/\delta}$. We incorporate this fact into our expression for $\mathrm{Im}f$ by writing

$$\frac{1}{kT}\mathrm{Im}f \cong \frac{A}{\xi^3}\left(\frac{x_0}{x}\right)^{7/3}\left(1+\frac{x}{x_0}\right)^{\phi}\exp\left[-\left(\frac{x_0}{x}\right)^2\right], \tag{2.21}$$

where

$$\phi = 10/3 + 1/\delta \cong 3.55. \tag{2.22}$$

Combining (2.14), (2.15), (2.19), and (2.21), we find the following expression for the nucleation rate:

$$J \cong A' \frac{D x_0^6}{\xi^5}\left(\frac{x}{x_0}\right)^{2/3}\left(1+\frac{x}{x_0}\right)^{\phi}\exp\left[-\left(\frac{x_0}{x}\right)^2\right], \tag{2.23}$$

where

$$A' \cong 1/288\pi\sqrt{3}\,. \tag{2.24}$$

The x-dependent prefactor that we have obtained in (2.23) is different from that derived by Binder and Stauffer[6], and the discrepancy possibly reflects an inherent limitation of the droplet model for the description of critical phenomena. As far as we can see, however, this part of the prefactor plays little or no role in nucleation kinetics; the results which we shall describe would remain qualitatively unchanged if we were to omit entirely the x-dependent part of the prefactor.

III. KINETIC EQUATIONS

Let the quantity $\nu(R)$ denote the distribution of B-phase droplets as a function of radius R. This distribution satisfies an equation of motion of the form

$$\frac{\partial \nu}{\partial t} = -\frac{\partial}{\partial R}[v(R)\nu(R)] + j(R), \tag{3.1}$$

where $v(R)$ is the radial velocity, dR/dt is given by the right-hand side of (2.10), and $j(R)$ is the distributed nucleation rate. That is, $j(R)$ is a distributed source of droplets such that

$$J = \int_{R^*}^{\infty} j(R)\,dR. \tag{3.2}$$

In the absence of $j(R)$, (3.1) is precisely the equation studied by Lifshitz and Slyozov.[7] In principle, we should introduce a specific function $j(R)$ and solve (3.1) directly. We have found it more interesting, at least as a first investigation, to develop an approximate procedure which allows us to obtain a great deal of information with a minimum amount of numerical analysis.

Our first major simplifying approximation—an important departure from Lifshitz and Slyozov—is to assume that only droplets with $R > R^*$ are to be counted as part of the B phase. We imagine $\nu(R)$ to look qualitatively as shown in Fig. 2. The shaded area to the right of R^* is N;

$$N = \int_{R^*}^{\infty} \nu(R)\,dR, \tag{3.3}$$

and droplets to the left of R^* are in the process of disappearing into the supersaturated A phase. Lifshitz and Slyozov interpret the entire area under the $\nu(R)$ curve as belonging to the B phase, and their interpretation is probably the more sensible one, especially for describing the late stages of a coarsening process. Our main reason for doing otherwise is that we simplify our mathematics; the cutoff at R^* allows us to deal only with the low-order moments of the sharply peaked shaded distribution rather than having to solve the complete partial differential equation (3.1). As hopeful justification for our device, we point out that we probably are not missing many droplets by neglecting the left-hand tail of the distribution, and that it is not clear in any case whether subcritical droplets are to be considered part of the emerging B phase or simply fluctuations in the parent A phase—especially during a stage of the process in which nucleation is still important.

Our equations of motion are obtained as follows. The time derivative of (3.3) produces

$$\frac{dN}{dt} = J - \nu(R^*)\frac{dR^*}{dt}, \tag{3.4}$$

and if we take the time derivative of

$$\bar{R} \equiv \frac{1}{N}\int_{R^*}^{\infty} \nu(R) R\,dR, \tag{3.5}$$

we find

$$\frac{d\bar{R}}{dt} = \langle v(R)\rangle + \frac{1}{N}\int_{R^*}^{\infty}(R-\bar{R})j(R)\,dR + (\bar{R}-R^*)\frac{\nu(R^*)}{N}\frac{dR^*}{dt}. \tag{3.6}$$

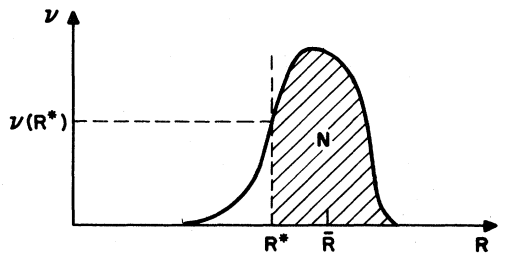

FIG. 2. Schematic distribution of droplets as a function of radius R.

The angular brackets in (3.6) denote an average with respect to $\nu(R)/N$, and we assume immediately that we can use (2.10) to write

$$\langle v(R)\rangle \cong v(\bar{R}) \cong (D\xi/3\bar{R}R^*)(1-R^*/\bar{R}). \tag{3.7}$$

The second term on the right-hand side of (3.6) can be written in the form

$$\left(\frac{d\bar{R}}{dt}\right)_{\text{nucleation}} \cong (J/N)(R^* - \bar{R} + \tfrac{1}{2}\delta R^*), \tag{3.8}$$

where δR^* is the width of the source distribution $j(R)$. Here we see an intrinsically stochastic question arising within a deterministic picture: at what point do dropletlike fluctuations become stable constituents of the B phase? We guess that the width δR^* corresponds to an uncertainty in the activation energy of the order of kT. That is,

$$\Delta E(R) \cong \Delta E^* - 4\pi\sigma\delta R^2; \tag{3.9}$$

thus

$$\delta R^* \cong (kT/8\pi\sigma)^{1/2} \equiv 4a\xi/x_0, \tag{3.10}$$

where

$$a \equiv \tfrac{1}{4}x_0(kT/8\pi\sigma\xi^2)^{1/2} \cong 1/(8\pi)^{1/2} \cong 0.2. \tag{3.11}$$

A final approximation is needed in order to evaluate $\nu(R^*)$. In situations where $\nu(R)$ is sharply peaked in the neighborhood of R^*, it seems reasonable to assume that the width of the shaded region in Fig. 2 is some constant multiple, say b^{-1}, of $\bar{R}-R^*$; thus we write

$$\nu(R^*) \cong Nb/(\bar{R}-R^*). \tag{3.12}$$

This assumption makes no sense, however, in a situation where the droplets have grown much bigger than R^*, that is, where appreciable growth has occurred but the supersaturation remains large enough that R^* is still small. In this case, we can say very little about the distribution near R^* except to guess that the terms containing $\nu(R^*)$ in (3.4) and (3.6) should be relatively unimportant because the main action is occurring elsewhere. We simply cut these terms off by writing

$$b = \begin{cases} b_0 & \text{for } \bar{R}-R^* \le \tfrac{1}{2}R^*, \\ 0 & \text{for } \bar{R}-R^* > \tfrac{1}{2}R^*. \end{cases} \tag{3.13}$$

The factor $\frac{1}{2}$ on the right-hand side of (3.13) is completely arbitrary. In fact, none of the more interesting results which we shall describe depends at all on the use of this cutoff. Without it, however, the unreasonably large coefficient of dR^*/dt in (3.6) causes dR^*/dt to diverge as the reaction goes to completion for small initial supersaturations x_1. To evaluate b_0, we shall insist that the long-time coarsening behavior of our theory match the Lifshitz-Slyozov result. Before showing how this works, it will be useful to summarize what we have done so far by writing down a complete and properly scaled version of our equations of motion.

The natural length scale for this problem is the correlation length ξ. For reasons which will become clear later, we define

$$y \equiv \frac{x}{x_0}, \quad \rho \equiv \frac{\bar{R}x_0}{2\xi}, \quad \rho^* \equiv \frac{R^*x_0}{2\xi} \cong \frac{x_0}{x} = \frac{1}{y}. \tag{3.14}$$

The correspondingly scaled time variable is

$$\tau \equiv Dx_0^3 t/24\xi^2. \tag{3.15}$$

If we write

$$n \equiv (64\pi\xi^3/x_0^3)N, \tag{3.16}$$

then the conservation condition (2.9) becomes

$$x_1 - x = n\rho^3, \tag{3.17}$$

and by virtue of (3.8) and (3.12), the equations of motion (3.4) and (3.6) become respectively

$$\frac{dn}{d\tau} = \tilde{J}(y) - \frac{nb}{(\rho-\rho^*)}\frac{d\rho^*}{d\tau}, \tag{3.18}$$

$$\frac{d\rho}{d\tau} = \frac{1}{\rho^2}\left(\frac{\rho}{\rho^*}-1\right) + \frac{\tilde{J}(y)}{n}(a-\rho-\rho^*) + b\frac{d\rho^*}{d\tau}, \tag{3.19}$$

where

$$\tilde{J}(y) \cong \tilde{A}y^{2/3}(1+y)^{3.55}\exp(-1/y^2), \quad \tilde{A} \cong 16/3\sqrt{3} \cong 3. \tag{3.20}$$

Note that all temperature-dependent quantities have disappeared in (3.17), (3.18), and (3.19); that is, we should be able to map the behavior observed at one temperature onto that at another simply by rescaling lengths and times according to (3.14) and (3.15). Eliminating n via (3.17), we find

$$\frac{d\rho}{d\tau} + \frac{\rho}{3}\left(\frac{1}{y_1-y} + \frac{b}{y(y\rho-1)}\right)\frac{dy}{d\tau} = -\frac{\rho^4\tilde{J}(y)}{3x_0(y_1-y)}, \tag{3.21}$$

$$\frac{d\rho}{d\tau} + \frac{b}{y^2}\frac{dy}{d\tau} = \frac{1}{\rho^2}(y\rho-1) + \frac{\rho^3\tilde{J}(y)}{x_0(y_1-y)}(a-\rho+1/y), \tag{3.22}$$

where $y_1 \equiv x_1/x_0$. These are the basic equations of our theory.

Consider now what happens if the nucleation terms are absent in (3.21) and (3.22), that is, when y becomes small enough that $\tilde{J}(y)$ is negligible and $b=b_0$. Equation (3.21) reduces to

$$\frac{3}{\rho}\frac{d\rho}{dy} = -\frac{1}{y_1-y} - \frac{b_0}{y(y\rho-1)}. \tag{3.23}$$

A simple analysis of (3.23) indicates that all trajectories in the ρ, y (or ρ, ρ^*) plane starting in the physical region $y < y_1$, $\rho > 1/y = \rho^*$, approach the

curve

$$\rho=(1+b_0/3)\rho^* \tag{3.24}$$

as y decreases (or ρ^* increases). (See Fig. 7 and the related discussion in Sec. IV.) Inserting (3.24) into (3.22), again with $\tilde{J}=0$, we find

$$3\rho^2\frac{d\rho}{d\tau}\approx b_0(3+b_0)/(3-2b_0). \tag{3.25}$$

Note that the familiar "$\tau^{1/3}$" law is recovered for any value of b_0 less than $\frac{3}{2}$. The Lifshitz-Slyozov value for the right-hand side of (3.25) is $\frac{4}{9}$, and we can reproduce this in our approximation by setting

$$b=0.317014. \tag{3.26}$$

To complete the theory, we must specify the initial conditions. Let us restrict our attention to shallow quenches from an equilibrated single-phase state, so that large critical fluctuations are already present in the system before the quench, and we do not have to be concerned about an incubation time for the nucleation rate. Then at $\tau=0$, we have $y=y_1$ and $n=0$. The only possible choice for ρ is

$$\rho(\tau=0)=a+1/y_1; \tag{3.27}$$

otherwise there is a nonintegrable singularity in the second term on the right-hand side of (3.22). This is physically reasonable; the first droplets emerge with $\bar{R}$ at the center of the distribution $j(R)$.

The theory summarized by Eqs. (3.21) and (3.22) contains a number of artificial features whose significance is hard to evaluate. We have checked that the numerical results to be described in Sec. IV are not strongly sensitive to the values chosen for a, b_0, or the cutoff defined in (3.13). On the other hand, we do not know whether the general form of, for example, Eq. (3.12) might be so seriously incorrect that it causes qualitative errors in our predictions. Nor do we know whether effects that we are ignoring altogether, such as coagulation of droplets when their density is high at large supersaturations, might turn out to be crucial. All we can say is that the effects we are considering—nucleation, growth, depletion, etc.—are real, and that we have made what seems to us to be a reasonable attempt to model them.

IV. NUMERICAL RESULTS

Numerical solutions of Eqs. (3.21) and (3.22) for various values of the initial supersaturation y_1 are shown in Figs. 3–7. These results have been obtained using standard forward-integration techniques. All calculations have been performed with $a=0.2$, $x_0=1.0$, and b as given in Eqs. (3.13) and (3.26).

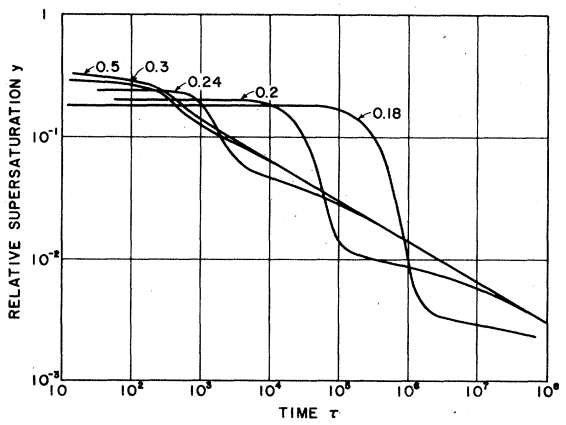

FIG. 3. Computed relative supersaturation y as a function of scaled time τ. Initial values y_1 are indicated for each curve.

Figure 3 is a log-log plot of the relative supersaturation y as a function of the scaled time τ. For initial supersaturations y_1 of the order 0.22 or smaller, that is, initial activation energies kT/y_1^2 of the order $20kT$ or greater, y remains unchanged during the early stage of droplet formation and growth. The reaction goes nearly to completion after a fairly well-defined y_1-dependent time delay, at which point y drops below its asymptotic $\tau^{-1/3}$ limit. The Lifshitz-Slyozov regime is not reached until very late in the process. In contrast, when y_1 is of the order of 0.3 or larger—the activation energy is $10kT$ or smaller—the $\tau^{-1/3}$ regime sets in almost immediately. This is the behavior that was described in the Introduction; nucleation is rapid but growth is slow, and droplets never become much larger than their capillarity-limited critical size.

When the initial supersaturation is larger than

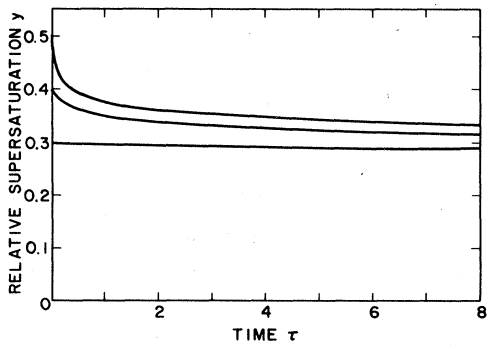

FIG. 4. Computed relative supersaturation y for small times τ and large initial y_1.

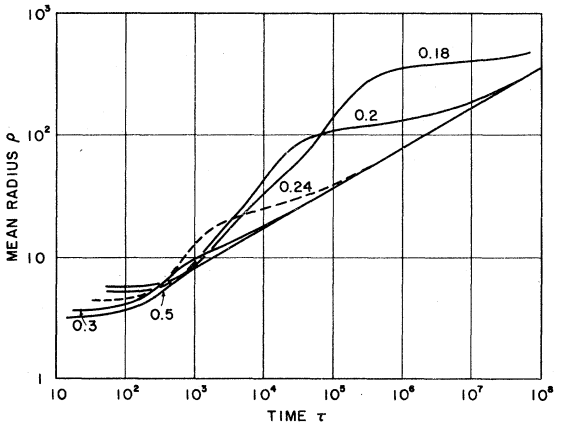

FIG. 5. Computed values of the scaled mean radius ρ as a function of time for various initial values of y_1 as indicated. The curve for $y_1 = 0.24$ is shown as a dashed line.

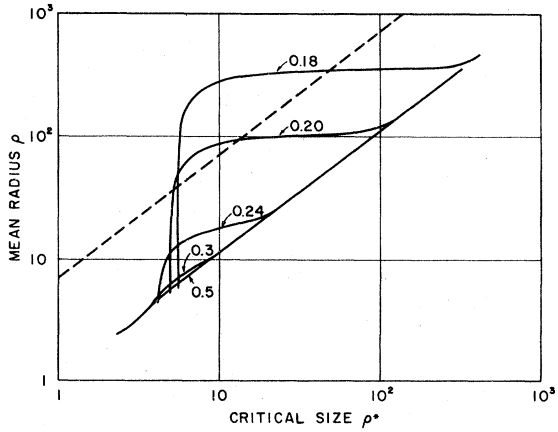

FIG. 7. Scaled mean radius ρ as a function of scaled critical size ρ^* for various initial values of y_1 as indicated. The dashed line indicates the Mullins-Sekerka stability limit at $\rho = 7\rho^*$.

approximately 0.3, our calculations indicate that y undergoes a downward transient which is completed within a time τ of the order of unity. This effect is shown in Fig. 4. The average droplet size remains essentially unchanged during this period, and the new phase emerges in the form of a large number of only marginally supercritical droplets. After this transient, the behavior of $y(\tau)$ is almost independent of the initial y_1, the main difference being that the density of droplets is larger for deeper quenches.

Figures 5 and 6 are log-log plots of dimensionless radius ρ and density n as functions of time τ. Here we see the characteristic features of shallow quenches ($y_1 \lesssim 0.22$); isolated, i.e., rare, droplets grow to be much larger than their critical size before the reaction goes any appreciable part of the way to completion. This behavior is illustrated more clearly in Fig. 7, where ρ is shown as a function of $\rho^* = 1/y$. [We may interpret the curves in Fig. 7 as the trajectories described following Eq. (3.23), except that here we have included the nucleation terms and have considered various values of y_1. Note the way that all trajectories approach the line $\rho \cong 1.106\rho^*$.] For values of y_1 less than about 0.21, ρ temporarily exceeds the Mullins-Sekerka limit[16] of $7\rho^*$ before the reaction slows. This means that the droplets may undergo a shape instability, possibly leading to faster and more intricate growth modes, before reverting to spheres under the influence of capillary forces during the final coarsening phase of the reaction. Figure 7 also can be used to deduce something about the width of the distribution $\nu(R)$. When ρ is close to ρ^*, that is, when we are in the $\tau^{1/3}$ regime, this distribution should have a width ΔR given by

$$\Delta R/\overline{R} \cong 2(\overline{R} - R^*)/\overline{R} \cong 0.2. \tag{4.1}$$

As we mentioned in the discussion following (3.12), we can say very little about ΔR for the case $\rho \gg \rho^*$. It seems safe to guess, however, that this width must exceed the estimate (4.1).

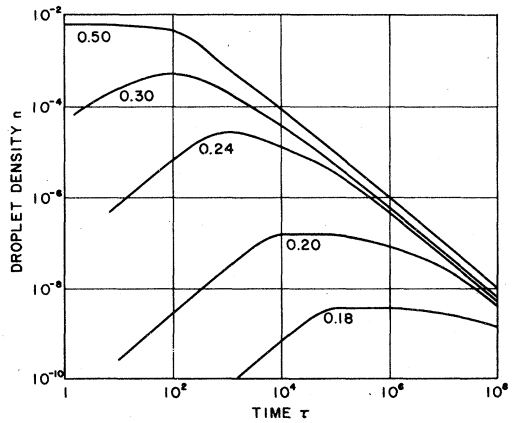

FIG. 6. Computed values of the scaled density of droplets, n, as a function of time τ for various initial values of y_1 as indicated.

Returning to Fig. 5, we note that the case of the intermediate quench, $y_1 = 0.24$, exhibits some features which are potentially important for experimental interpretation. Except during the extreme late stage, no simple power-law behavior is apparent. The period of free growth at constant y, which should produce a $\tau^{1/2}$ law [see Eq. (4.3)], occurs somewhere in the neighborhood of $\tau = 10^3$, but lasts for less than a decade. There follows, for a decade or more, a period of slow growth which might look as if it were characterized by a power law $\tau^{a'}$, with $a' < \frac{1}{3}$, but which is better under-

stood as a transition period with no special algebraic signature. The lesson here is that power-law analysis can be quite misleading, even in what may appear to be the late stages of a coarsening process.

In order to make comparisons with previous analyses, we have drawn in Fig. 8 a semilog plot of the time τ_c at which the reaction is halfway to completion, $y(\tau_c)=\frac{1}{2}y_1$, as a function of y_1. (We refer to τ_c simply as the "completion time.") Note the shoulder in this curve in the neighborhood of $y_1 \cong 0.24$ which marks the transition between the two types of behavior described above.

The dashed curve in Fig. 8 is the completion time obtained by making the Binder-Stauffer approximation but retaining the same nucleation and scaling formulas that we have used elsewhere in the present paper. Specifically, we assume that y remains fixed at y_1 for purposes of estimating rates of nucleation and growth, and that the capillary correction to the growth rate is negligible because droplets become very large as the reaction goes to completion. That is,

$$\frac{dn}{d\tau} \cong \tilde{J}(y_1) \tag{4.2}$$

and

$$\frac{d\rho}{d\tau'} \cong y_1/\rho, \quad \rho(\tau') \cong (2y_1\tau')^{1/2}, \tag{4.3}$$

where τ' denotes time after formation, and the formation radius, $\rho(0) \cong \rho^*$, is assumed to be relatively small. In this approximation new droplets are formed at a constant rate throughout the process; thus

$$y_1 - y(\tau) \cong \frac{\tilde{J}(y_1)}{x_0} \int_0^\tau (2y_1\tau')^{3/2}\, d\tau'$$
$$= (2/5x_0)\tilde{J}(y_1)(2y_1)^{3/2}\tau^{5/2}. \tag{4.4}$$

Setting $y(\tau_c)=\frac{1}{2}y_1$, we find

$$\tau_c \cong [25x_0^2/128y_1\tilde{J}^2(y_1)]^{1/5}, \tag{4.5}$$

which with $x_0=1.0$ is the relation shown in Fig. 8. As expected, the Binder-Stauffer theory agrees reasonably well with ours for y_1 less than approximately 0.2.

The quantity which ordinarily has been computed in nucleation theory is not the completion time but a nucleation time, the latter being defined typically as the time required for a droplet to form in one cubic centimeter of supercooled fluid. This time t_N is simply equal to $1/J$, where J is the nucleation rate in (2.23). Unfortunately there is no simple scaled version of t_N. In accord with (3.15), we write that

$$\tau_N \equiv Dx_0^3 t_N/24\xi^2 \cong 64\pi\xi^3/\tilde{J}(y_1). \tag{4.6}$$

The dash-dot curve in Fig. 8 is obtained from (4.6) with $\xi=10^{-6}$ cm, a value which is typical of correlation lengths in fluids at $\epsilon \cong 10^{-3}$. The almost vertical slope of this curve is the basis for the assertion that nucleation theory predicts a limit of supersaturation at about $x_1=0.13$ which is very nearly temperature independent and is not even sensitive to most other parameters in the theory. For example, if we were to change the definition of t_N so as to require 10^5 nuclei per cubic centimeter instead of just one, we would shift the nucleation curve in Fig. 8 to the right by only $\Delta y_1=0.01$. The crucial point is that the nucleation curve lies markedly to the left of the completion curve for physically accessible values of τ_c.

The scaling properties of the completion curve suggest that we modify the usual scheme for presentation of experimental results so as to be able to superimpose data from a variety of different substances. If we choose a fixed completion time t_c, say 10 or 100 sec, which characterizes our observational technique, then the scaling law

$$\tau_c(y_1) = Dx_0^3 t_c/24\xi^2 = ([D]x_0^3 t_c/24[\xi]^2)\epsilon^{3\nu} \tag{4.7}$$

becomes a relation between the relative supersaturation y_1 and temperature ϵ. Rescaling of ϵ according to

$$\epsilon_c \equiv ([D]x_0^3/24[\xi]^2)^{1/3\nu}\epsilon \tag{4.8}$$

leads to the law

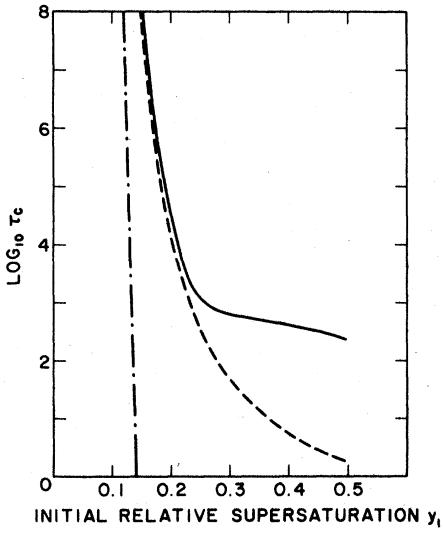

FIG. 8. Half-completion time τ_c as a function of initial relative supersaturation y_1. The solid line is the present theory. The dashed curve has been computed using the Binder-Stauffer approximation, and the dash-dot curve is the conventional nucleation time.

$$\epsilon_c^{3\nu}=\tau_c(y_1)/t_c\,. \tag{4.9}$$

It now should be clear why the factors of x_0 were included in the scale transformations (3.14)–(3.16). The only possibly system-dependent parameter in (4.9) is x_0, which enters $\tau_c(y_1)$ because it appears explicitly in the equations of motion (3.21) and (3.22). In those equations, however, x_0 occurs only in conjunction with $\tilde{J}$, whose amplitude might contain other x_0-dependent factors and which, in any case, is uncertain to at least one order of magnitude. Furthermore, a quantity like $\log_{10}\tau_c$ will be insensitive to small variations in the amplitude of $\tilde{J}$. Thus even if x_0 is not a universal constant, it should be accurate to delete the explicit x_0 in (3.21) and (3.22), and to regard the resulting τ_c as a universal function of the relative supersaturation $y_1=x_1/x_0$. To summarize: If a certain class of measurements is characterized by a fixed observation time t_c and if all of our scaling assumptions are correct, then all such measurements of, say, maximum relative supersaturation y_1 should lie on a single curve $y_1(\epsilon_c)$, as given implicitly by (4.9).

V. COMPARISON WITH EXPERIMENT

The present experimental situation is, to say the least, unsettled. Relevant data exist for three systems, each of which is reputed to exhibit a nucleation-rate anomaly near its critical point. Of these systems, two are binary fluid mixtures: C_7H_{14}-C_7F_{14} (Refs. 1 and 2) and 2, 6-lutidine-water[4]; and one is a pure substance: CO_2 (Ref. 3). The observations are all cloud-point measurements which, in principle, determine maximum attainable supersaturation x_1 as a function of temperature ϵ. The data are shown in Fig. 9 in the form of the y_1 vs ϵ_c plot described in the final paragraph of Sec. IV. Also shown in this figure are the completion curves for t_c =1, 10 and 100 sec.

It is important to understand the different assumptions and uncertainties associated with each of the three sets of data points shown in Fig. 9. We discuss these cases separately.

a. 2, 6-lutidine-water[4] (solid circles). The most recent of the three experiments, this is the only one which really penetrates the near-critical region where we expect the transition to be shifted to larger values of the supersaturation. The data do indicate such a shift, but a number of experimental points remain to be clarified. The lutidine-water system has a lower critical solution point, and "quenches" were performed by pulsed heating via microwave radiation. The cloud point was identified as the quench depth at which there occurred a sharp increase in the attenuation of a laser beam passing through a thin section of the sample. Total quench times are reported to have been of the order of tens of seconds, but the detailed thermal history of each quench was significantly different from the simple single-step model that we have used in our calculations. Moreover, there is not necessarily any simple, temperature-independent relation between the half-completion times that we have calculated and the onset of observable attenuation of a laser beam.

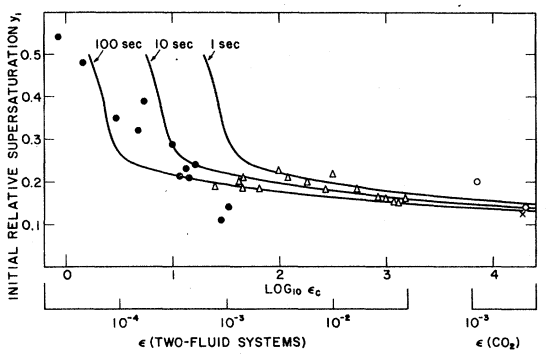

FIG. 9. Experimental cloud-point data. The points indicate values of initial relative supersaturation y_1 vs scaled temperature ϵ_c as defined in Eq. (4.8). Solid circles denote 2, 6-lutidine-water (Ref. 4), open triangles denote C_7H_{14}-C_7F_{14} (Ref. 2), and open circles denote CO_2 (Ref. 3). Also shown are completion curves for t_c =1, 10, and 100 secs.

None of the thermodynamic quantities necessary for calculating activation energies are known for this system; thus we have no independent estimate of x_0 and have simply set x_0= 1.0. If x_0 is larger than unity, as seems to be the case for other systems, then the solid circles in Fig. 9 should be shifted downward. The quantities relevant to the kinetic factor [Eq. (4.8)] have been measured[17] to be $[D]\cong 2\times10^{-6}$ cm^2/sec, $[\xi]\cong 2\times10^{-8}$ cm, and $\nu'\cong 0.62$. Thus

$$\log_{10}\epsilon_c\cong\log_{10}\epsilon+4.48. \tag{5.1}$$

b. C_7H_{14}-C_7F_{14}: (open triangles). This is the system for which the nucleation-rate anomaly was first detected.[1] Heady and Cahn[2] have provided us with a wealth of thermodynamic information about this system, including an indirect evaluation of $\partial\mu/\partial C$. We have reanalyzed their data using modern scaling notation and find

$$\left[\frac{\partial\mu}{\partial C}\right]\cong(1.03\pm0.1)\times10^{-33}\ \text{erg cm}^3, \tag{5.2}$$

$$[\sigma]\cong 21.9\ \text{erg cm}^{-2}, \tag{5.3}$$

and

$$[\Delta C]\cong 3.12\times10^{21}\ \text{cm}^{-3}. \tag{5.4}$$

Critical indices are $\gamma' \cong 1.25$, $\nu' \cong 0.62$, and $\beta \cong 0.31$. We also need to know that T_c is 319 K. Then using Eqs. (2.11) and (2.18) we find

$$x_0 \cong 1.30 \pm 0.1. \tag{5.5}$$

Unfortunately we have no information at all about the diffusion constant. We have simply used (5.1) to locate the data along the ϵ_c axis; but because we are dealing with relatively large and slowly diffusing molecules, it is possible that the experimental points in Fig. 9 should be displaced appreciably to the left. Cloud points were observed visually, and the cooling rate is reported to have been adjusted so that total quench times were always of the order of several minutes.

c. CO_2 (open circles). Data are shown here for only the two most nearly critical CO_2 samples tested by Huang *et al.*[3] Other points lie off the right-hand edge of the graph, well below the completion curves. We have reevaluated x_0 using the value of Herpin and Meunier[18] for the surface tension:

$$[\sigma] \cong 95.1 \pm 10 \text{ erg cm}^{-2} \tag{5.6}$$

and

$$\left[\frac{\partial \mu}{\partial n}\right] \cong 1.33 \times 10^{-34} \text{ erg cm}^3, \tag{5.7}$$

which is deduced from data published by Swinney and Henry.[19] The symbol n denotes the number density in (5.7). Other parameters are the same, as shown in Ref. 14. The resulting x_0 is

$$x_0 \cong 1.24 \pm 0.1, \tag{5.8}$$

which is about 50% larger than our earlier estimate.[14]

According to Eq. (6.34) in Ref. 14, the quantity that plays the role of the diffusion constant D for the pure substance is[20]

$$\hat{D} \equiv \frac{\lambda T_c (\Delta n)^2}{l^2 n_c^2} \left(\frac{\partial \mu}{\partial n}\right), \tag{5.9}$$

where λ is the thermal conductivity, l the latent heat per molecule, and n_c the critical number density. From Table IIB in Ref. 19 we deduce that

$$\lambda \cong 6.5 \times 10^2 \epsilon^{\nu' - \gamma'} \text{ erg cm}^{-1} \text{ sec}^{-1} \text{ K}^{-1} \tag{5.10}$$

and thus

$$\hat{D} \cong 5.2 \times 10^{-4} \epsilon^{\nu'} \text{ cm}^2 \text{ sec}^{-1}. \tag{5.11}$$

Finally, using[18] $[\xi] = 0.714 \times 10^{-8}$ cm and $\nu' = 0.63$, we find

$$\log_{10} \epsilon_c \cong \log_{10} \epsilon + 6.80. \tag{5.12}$$

Cloud points were observed in these samples by a calorimetric technique in which it was possible to check that the total latent heat released was thermodynamically consistent with the directly measured undercooling. Total quench times were of the order of minutes or longer. In Fig. 9, X indicates a point ($\epsilon = 3.15 \times 10^{-3}$, $x_1 = 0.16$) where the sample was held for more than four hours without appreciable loss of latent heat.

The overall picture which emerges in Fig. 9 is not one of dramatic, systematic disagreement between theory and experiment. The lutidine data, while scattered, lie on or below the 10-sec completion curve which should be the appropriate time scale for that particular experiment. Some of the Heady-Cahn results lie a bit higher in y_1 than expected, but these discrepancies are well within the uncertainties in x_0 and ϵ_c. It seems to us that the only remaining evidence for a nucleation-rate anomaly, that is, for excess stability, resides in the single CO_2 cloud point at $\epsilon \cong 1.13 \times 10^{-3}$, $y_1 = 0.202$. This is not to say that apart from this point we have achieved credible agreement between theory and experiment, but we hope that we may have discovered some clues about where to look for such agreement. In this regard, it should be emphasized that data obtained for $\tau \leq \tau_c$ with relative supersaturations y_1 less than about 0.24 will fall within the region where our theory is consistent with the Binder-Stauffer approximation and thus where our predicted values of $n(\tau)$, $\rho(\tau)$, etc. are not very sensitive to the special assumptions introduced in Sec. III. This region includes almost all of the data shown in Fig. 9 except for the lutidine-water results. Direct measurements of numbers and sizes of droplets ought to be feasible in this region and information at this level of detail ought to tell us, finally, whether there really is something strange and interesting happening in these systems.

ACKNOWLEDGMENT

This work was supported by AFOSR Grant No. F 44620-76-0103.

[1] B. E. Sundquist and R. A. Oriani, J. Chem. Phys. 36, 2604 (1962).
[2] R. B. Heady and J. W. Cahn, J. Chem. Phys. 58, 896 (1973).
[3] J. S. Huang, W. I. Goldburg, and M. R. Moldover, Phys. Rev. Lett. 34, 639 (1975).
[4] A. J. Schwartz, S. Krishnamurthy, and W. I. Goldburg (unpublished).
[5] J. Frenkel, *Kinetic Theory of Liquids* (Dover, New York, 1955), Chap. VII.

[6]K. Binder and D. Stauffer, Adv. Phys. 25, 343 (1976).
[7]I. Lifshitz and V. Slyozov, J. Phys. Chem. Solids 19, 35 (1961).
[8]J. S. Langer, in *Fluctuations, Instabilities and Phase Transitions*, edited by T. Riste (Plenum, New York, 1975).
[9]H. E. Stanley, *Introduction to Phase Transitions and Critical Phenomena* (Oxford University, New York, 1971).
[10]J. S. Langer, Ann. Phys. (N.Y.) 41, 108 (1967).
[11]J. S. Langer, Ann. Phys. (N.Y.) 54, 258 (1969).
[12]S. Coleman, Phys. Rev. D 15, 2929 (1977).
[13]C. G. Callan and S. Coleman, Phys. Rev. D 16, 1762 (1977).
[14]J. S. Langer and L. A. Turski, Phys. Rev. A 8, 3230 (1973).
[15]N. J. Günther, D. A. Nicole, and D. J. Wallace (unpublished).
[16]W. W. Mullins and R. F. Sekerka, J. Appl. Phys. 34, 323 (1963).
[17]E. Gulari, A. F. Collings, R. L. Schmidt, and C. J. Pings, J. Chem. Phys. 56, 6169 (1972).
[18]J. C. Herpin and J. Meunier, J. Phys. (Paris) 35, 847 (1974).
[19]H. L. Swinney and D. L. Henry, Phys. Rev. A 8, 2586 (1973).
[20]We should take this opportunity to correct an error in Ref. 14. Equation (6.24) in that paper is missing a factor $n_l/\Delta n$, and, as a result, Δn should be replaced by n_l in Eq. (6.34) and elsewhere. This correction makes very little difference in the numerical results, but without it the theory does not scale properly in ϵ.